ELSEVIER

Polymer 40 (1999) 2303–2312

polymer

Thermal and mechanical properties of poly(L-lactic acid)–poly (ethylene-*co*-vinyl acetate) blends[1]

Jin-San Yoon[a,*], Sung-Hwan Oh[a], Mal-Nam Kim[b], In-Joo Chin[a], Young-Ha Kim[c]

[a]*School of Chemical Science and Engineering, Inha University, Inchon 402-751, South Korea*
[b]*Department of Biology, Sangmyung University, Seoul 110-743, South Korea*
[c]*Korea Institute of Science and Technology, Cheongrang, Seoul 130-650, South Korea*

Received 15 August 1997; revised 19 May 1998; accepted 19 May 1998

Abstract

Poly(L-lactic acid)(PLLA) was blended with poly(ethylene-*co*-vinyl acetate)(EVA) and the miscibility of the blend was investigated by DSC, polarizing optical microscopy and rheometry. The blend of PLLA with EVA70, that contained 70 wt% of vinyl acetate, was immiscible because the T_g and the spherulitic growth rate of the blend were nearly constant regardless of the change in the blend composition. On the other hand, the T_g, equilibrium melting temperature, the spherulitic growth rate during the isothermal crystallization of the PLLA–EVA85 blend were decreased with the increase in the EVA content. Moreover, the Flory–Huggins interaction parameter of the blend was found to be negative, which clearly means the PLLA–EVA85 blend was miscible. The tensile strength and modulus of the PLLA–EVA85 blend were dropped rapidly, followed by a more gradual decrease with the increase in the EVA85 content. Strain-at-break, however, was increased rather slowly up to 70 wt% of EVA85 and then increased quite rapidly around 90 wt% of EVA85.

Keywords: Poly(L-lactic acid); Poly(ethylene-*co*-vinyl acetate); Miscibility

1. Introduction

Poly(L-lactic acid)(PLLA) degrades biologically into lactic acid, a product of the carbohydrate metabolism, and its importance as a substitute for the non-degradable thermoplastics has attracted a lot of attention in recent years. Poly(lactic acid)(PLA) exists in L- and D-form, which are optical isomers. PLA with large amount of L-form isomer is highly crystalline. In general, the crystallinity and biodegradability depend on the content of D-form isomer [1]. Thanks to its biocompatibility PLLA is suitable for sutures [2,3], drug delivery systems [4,5], and implants for bone fixation [6].

Since PLLA is very brittle at room temperature and hydrolyzes easily, its applicability has been limited [7–11]. Several studies on blending or copolymers of PLLA have been reported in order to modify the properties and biodegradability [12–19].

Poly(vinyl acetate) has been shown to be miscible with PLLA [16], and we have investigated the miscibility of PLLA with poly(ethylene-*co*-vinyl acetate)(EVA) containing 70 and 85 wt% of vinyl acetate unit. The themal and mechanical properties of the blend were explored.

2. Experimental

2.1. Materials

Condensation polymerization of lactic acid with dipentaerythritol(0.1 wt%) produced star-shaped PLLA. PLLA was precipitated in methanol and dried before use. EVA70, that contained 70 wt% vinyl acetate, was purchased from Scientific Polymer Products and EVA 85, that contained 85 wt% vinyl acetate, was provided in latex form by Taeyoung Chemical Co. The surfactant was removed by the soxhlet extraction for 1 week in methanol. The chloroform soluble fraction of EVA85 was used for the blending. The composition of the copolymer was confirmed by ^{1}H-n.m.r. Table 1 shows the molecular characteristics of the raw materials.

2.2. Blending

PLLA and EVA were dissolved in chloroform (3 wt%), and they were blended with stirring to form a uniform solu-

* Corresponding author.

[1]Dedicated to Prof. Ick-Sam Noh on the occasion of his retirement from Inha University.

0032-3861/99/$ - see front matter
PII: S0032-3861(98)00463-7

Table 1
Characteristics of polymers

Polymer	Structural formula	$\overline{M}_w$[a]	vinyl acetate content[b] (wt%)
PLLA	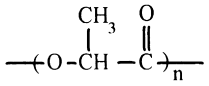	41 900	-
EVA70	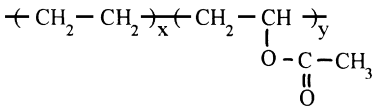	285 000	69.1
EVA85		646 000	85.8

[a]Measured by g.p.c. in chloroform at 30°C. [b]Measured by ^{1}H-n.m.r.

tion. Film samples were obtained by initially drying the solution at ambient temperature, followed by drying under vacuum at 40°C. The films were compacted in a hot press at 150°C and 250 atm for 1 min.

2.3. Analysis

The melting temperature was obtained by heating the sample from room temperature to 165°C at a rate of 10°C min^{-1}, holding it at 165°C for 1 min, cooling it to room temperature at 10°C min^{-1}, and then reheating it to 165°C. The equilibrium melting temperature was estimated by heating the sample to 165°C at a rate of 10°C min^{-1}, holding it at 165°C for 1 min, quenching it to the predetermined crystallization temperature(T_c) at a rate of −200°C min^{-1}, recrystallizing it at T_c for 120 min, and then reheating it at 10 °C min^{-1}.

E', E'' and tanδ of the film (50 × 4 × 0.03 mm) were measured using a Rheovibron (DDV-II-C) at a fixed

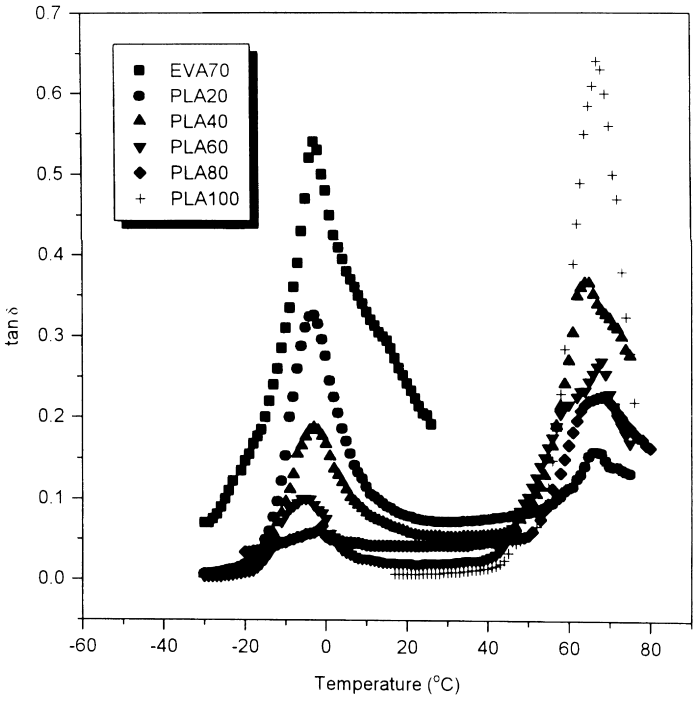

Fig. 1. Tanδ curve of PLLA–EVA70 blends.

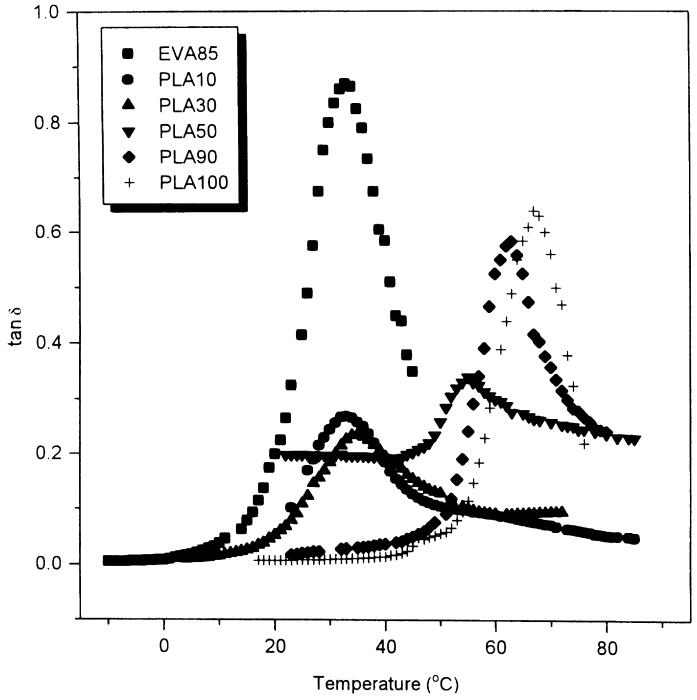

Fig. 2. Tanδ curve of PLLA–EVA85 blends.

frequency of 11 Hz while heating the sample from −30°C at a heating rate of 10°C min^{-1}.

The spherulitic growth rate in the blend films was determined using a polarizing microscope (Nikon OPTIPHOT2-POL). The sample was heated to 165°C for 1 min, and then quenched to the pre-determined T_c, at a rate of −100°C min^{-1} before being observed with a CCD camera. The microscopic heterogeniety of the blend was investigated using a Rheometer (Physica MC-120). Cone-and-plate geometry was used in the frequency range of 0.16–10 Hz. Mechanical properties of the film were measured with a tensile testing machine (Lloyde Instrument, LR 5OK) at a crosshead speed of 50 mm min^{-1} according to ASTM D882-90. The load cell used had a maximum range of 2.5 KN, the

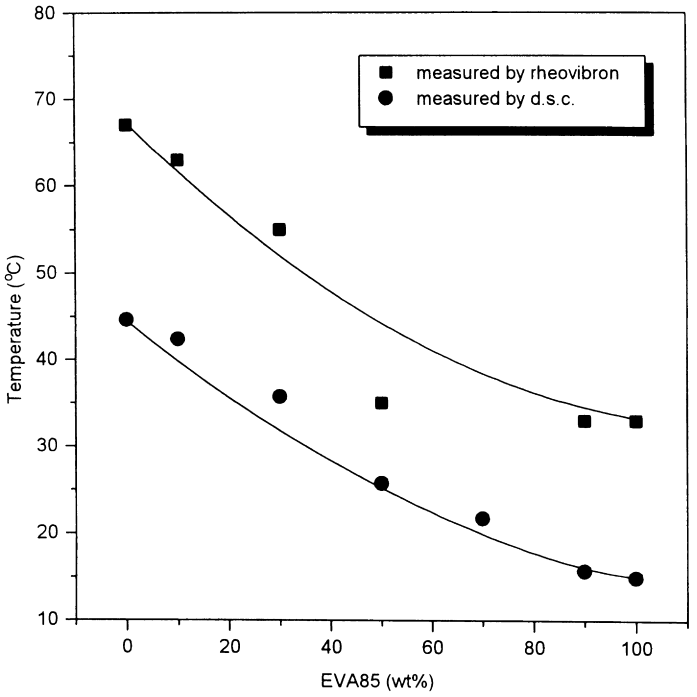

Fig. 3. Glass transition temperatures of PLLA–EVA85 blend.Solid line: the Fox equation results.

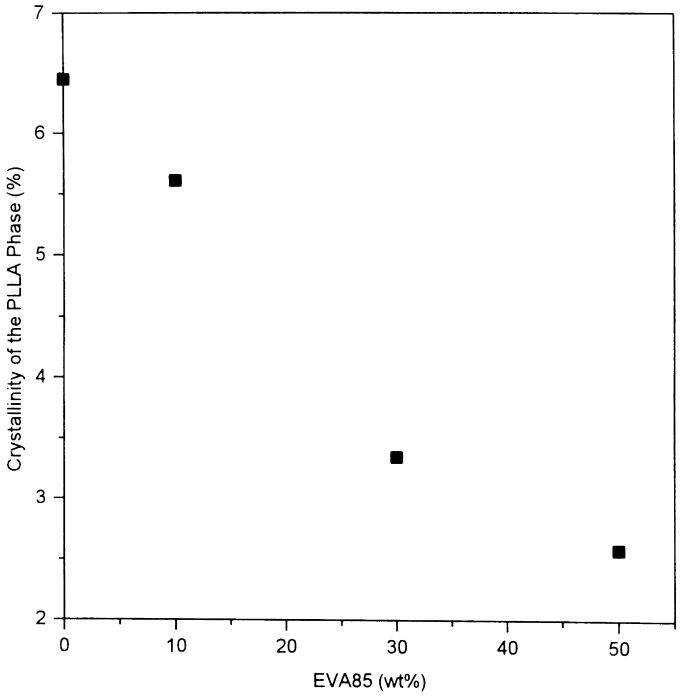

Fig. 4. Crystallinity of the PLLA–EVA85 blends measured by DSC.

sample gauge length was 50 mm, and the sample width was 10 mm.

3. Results and discussion

Fig. 1 shows tanδ as a function of temperature for the PLLA–EVA70 blends, as determined by Rheovibron. Two separate glass transition peaks, each due to the respective constituent polymer, are clearly seen and they were independent of the blend composition. Thus, we may deduce PLLA and EVA70 are not compatible. On the other hand, the PLLA–EVA85 blend shows a single glass transition peak in Fig. 2, which is located between the T_g of PLLA and the T_g of EVA 85. The transition peak of the PLLA–EVA85 blend was also dependent upon the blend composition.

The glass transition temperature obtained from the Rheovibron measurements is in general at a higher temperature

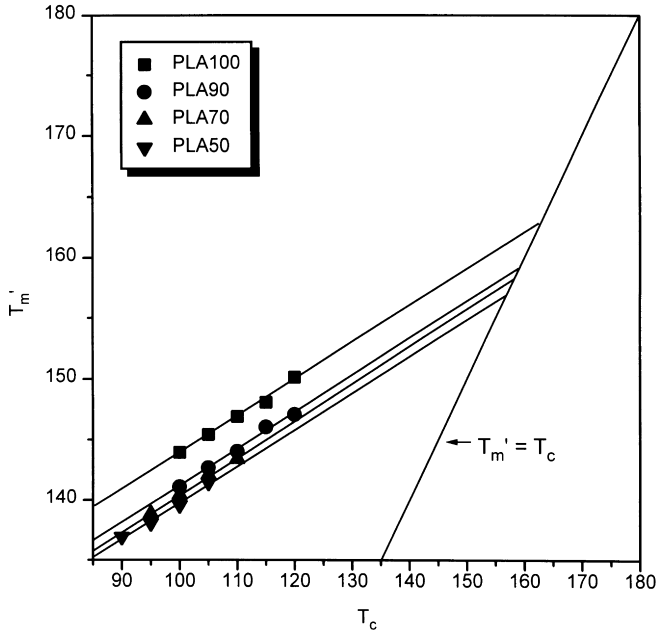

Fig. 5. Observed melting temperature (T_m') as a function of crystallization temperature (T_c) for PLLA–EVA85 blends.

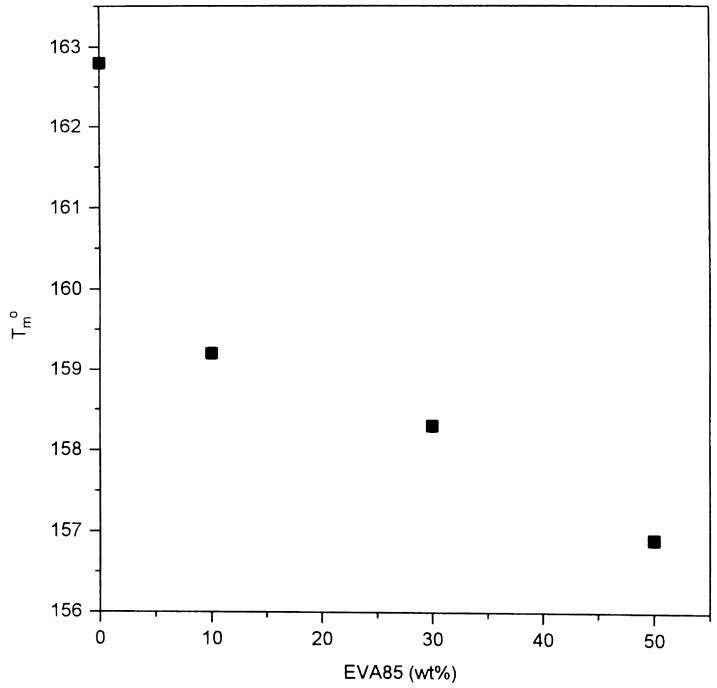

Fig. 6. Equilibrium melting temperature of PLLA–EVA85 blends.

than that determined by DSC. The solid line in Fig. 3 is the calculated T_g, based on the following equation proposed by Fox [20].

$$\frac{1}{T_g} = \frac{W_{PLLA}}{T_{g,PLLA}} + \frac{W_{EVA85}}{T_{g,EVA85}} \quad (1)$$

where W is the weight fraction, and the subscript indicates the constituent of the blend. Fig. 3 clearly shows that the agreement between the experimental T_g of the PLLA–EVA85 blend and the theoretical T_g is as good as the agreement for the miscible PLLA–PVAc blend [16]. The samples for the T_g determination by DSC and Rheo-

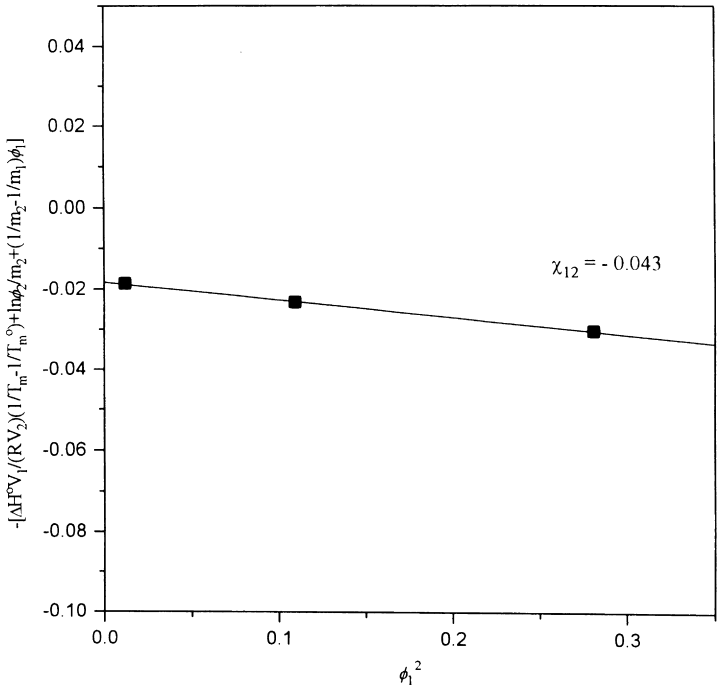

Fig. 7. Melting-point depression for PLLA–EVA85 blends and the Flory–Huggins equation results.

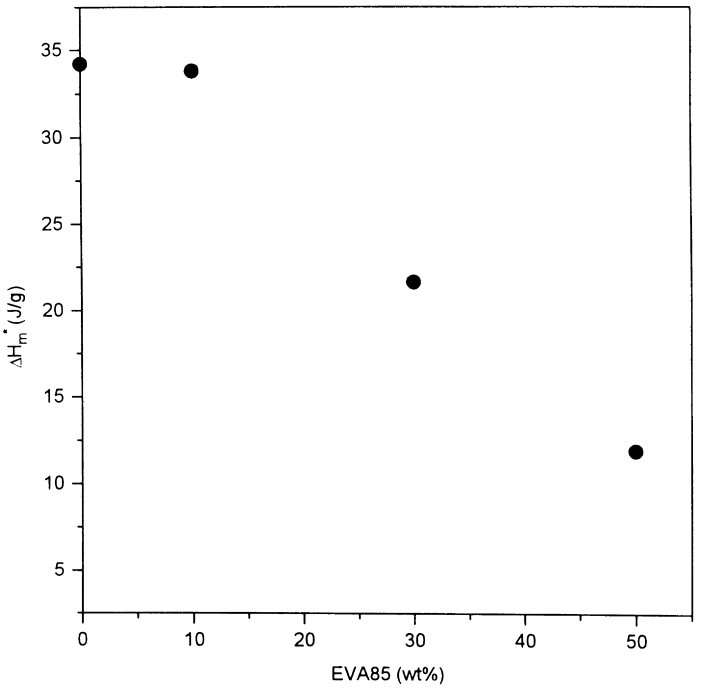

Fig. 8. Non-isothermal 2nd scan overall enthalpy of fusion based on the unit weight of PLLA in the blends (ΔH_m^*).

vibron were prepared by quenching at a rate of $-200\ ^\circ C\ min^{-1}$ after melting at 165 °C for 1 min, and by pressing at 150 °C, 250 atm followed by quenching. Therefore, the two polymers are believed to be miscible in the melt state.

The crystallinity of PLLA in the blend can be calculated by the following equation.

$$X_c = \frac{\Delta H_m^*}{\Delta H^o} \tag{2}$$

where ΔH^0 is the heat of fusion per unit weight of the perfectly crystalline PLLA, and ΔH_m^* is the heat of fusion

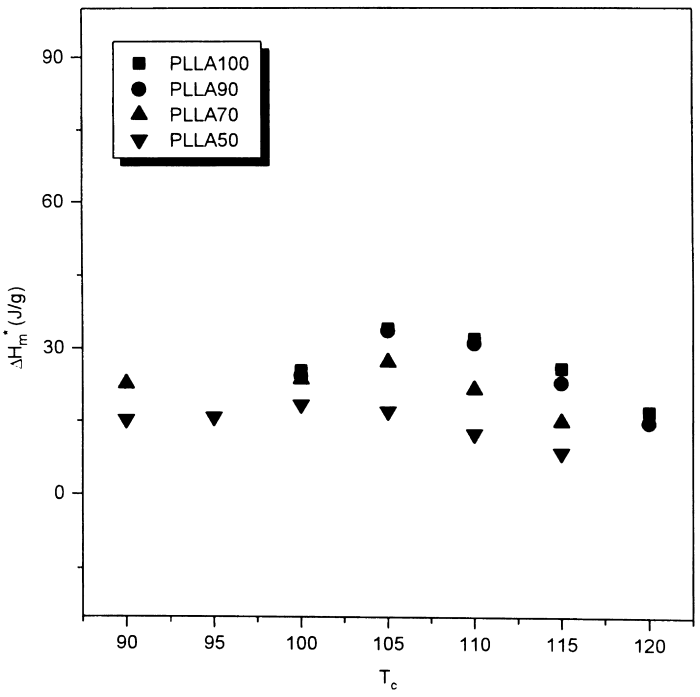

Fig. 9. Enthalpy of fusion determined during the measurement of the equilibrium melting temperature based on the unit weight of PLLA in the blends as a function of T_c.

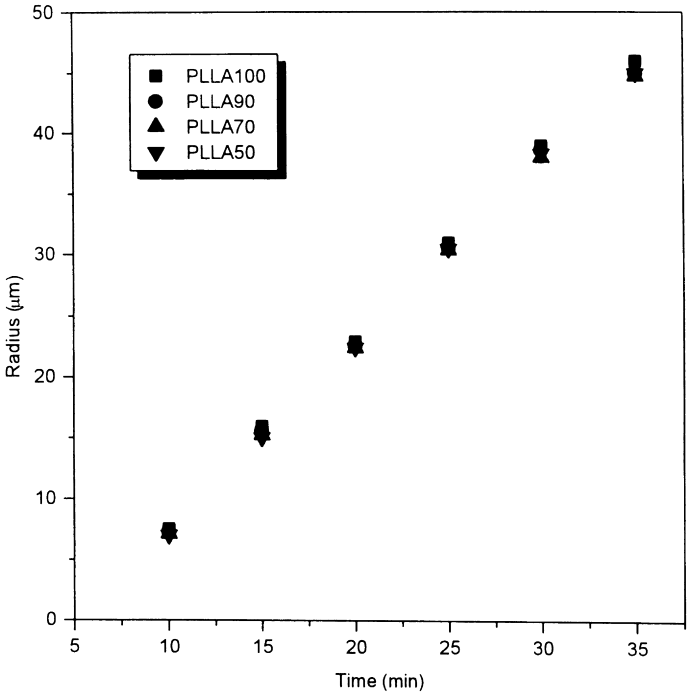

Fig. 10. Radius of PLLA spherulites in the PLLA–EVA70 blends as a function of time at $T_c = 105$°C.

per unit weight of PLLA, that can be calculated from the heat of fusion of the blend (ΔH_m) as follows

$$\Delta H_m^* = \frac{\Delta H_m}{\text{PLLA content (wt\%)}} \times 100 \quad (3)$$

Thus, the crystallinity of PLLA in the PLLA–EVA85 blend was obtained by utilizing the heat of fusion of the blend, which was determined by DSC, and was plotted in Fig. 4. As the content of EVA85 in the blend was increased, the crystallinity of PLLA was drastically reduced.

The equilibrium melting temperature, which can be

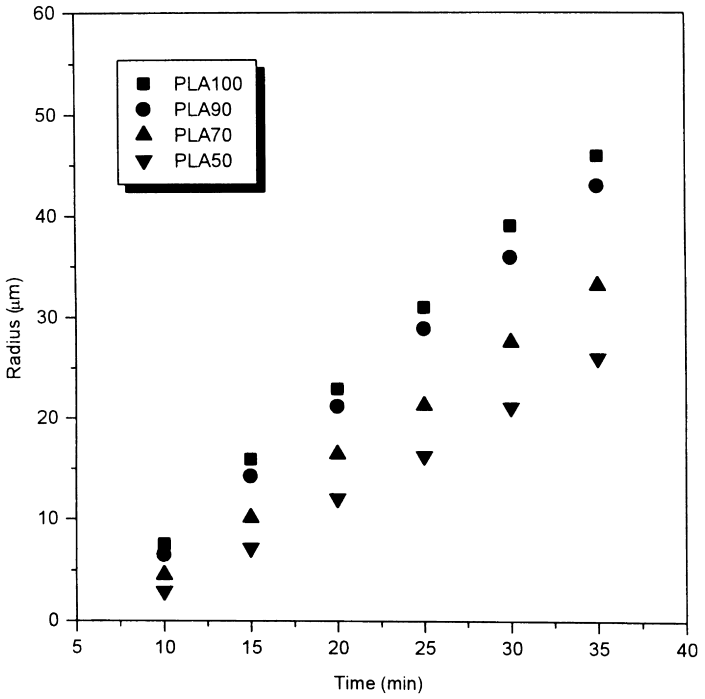

Fig. 11. Radius of PLLA spherulites in the PLLA–EVA85 blends as a function of time at $T_c = 105$°C.

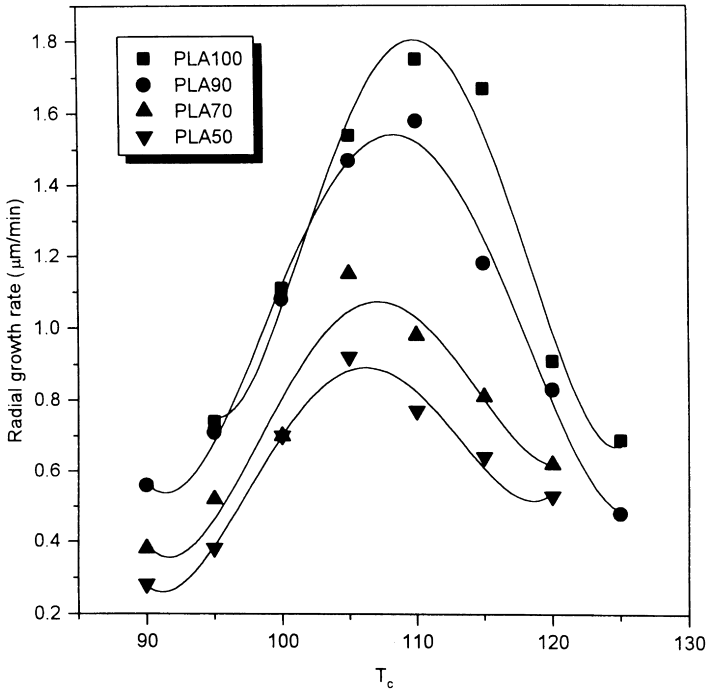

Fig. 12. Radial growth rate of spherulite as a function of crystallization temperature for PLLA–EVA85 blends.

defined as the fusion temperature of the infinitely large lamella, can be obtained by the following Hoffman–Weeks equation [21].

$$T_m' = \frac{T_c}{\gamma} + (1 - \frac{1}{\gamma})T_m^o \quad (4)$$

where T_m' is the observed melting temperature, T_c is the crystallization temperature, T_m^o is the equilibrium melting temperature, and γ is the ratio of the initial to the final lamellar thicknesses. The value of γ lies between 0 and 1. In Fig. 5 the observed melting temperature was determined by heating the blend specimen to 165°C at a rate of 10°C min^{-1}. Each specimen was previously heated from room temperature to 165°C at 10°C min^{-1}, being held at 165°C for 1 min, and then crystallized for 120 min by quenching from 165°C at −200°C min^{-1} to the

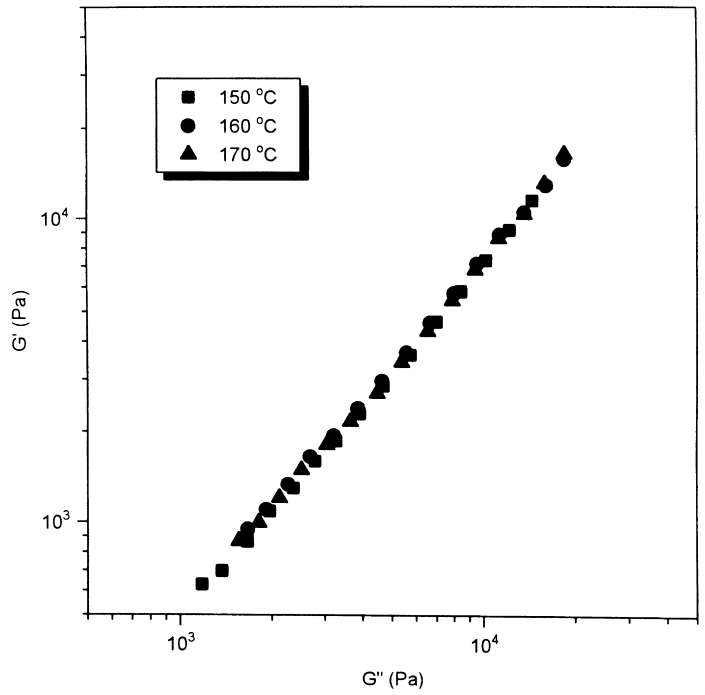

Fig. 13. Plot of logG' versus logG'' for PLLA–EVA85 (50/50) at various temperatures.

predetermined crystallization temperature. The equilibrium melting temperature was then obtained by extrapolating the melting temperature to $T_m = T_c$. In Fig. 6 the equilibrium melting temperature was decreased with an increase in the EVA85 content in the blend, which indicates the constituent polymers in the blend were thermodynamically miscible.

According to the Flory–Higgins theory [22], [23], the depression of the equilibrium melting temperature can be descibed as follows

$$\frac{1}{T_m} - \frac{1}{T_m^o} = -\frac{RV_2}{\Delta H^o V_1}\left[\frac{\ln\phi_2}{m_2} + \left(\frac{1}{m_2} - \frac{1}{m_1}\right)\phi_1 + \chi_{12}\phi_1^2\right] \quad (5)$$

where χ_{12} is the interaction parameter between the constituents of the blend, V is the molar volume of the repeat unit at the equilibrium melting temperature, ϕ is the volume fraction of the constituent in the blend, m is the degree of polymerization, ΔH^o is the heat of fusion of the perfect crystalline polymer and T_m and T_m^o are the equilibrium melting temperature of the blend and the crystalline constituent, respectively. Subscripts 1 and 2 represent the noncrystalline and the crystalline constituents, respectively. Eq. (5) can be rearranged as

$$-\left[\frac{\Delta H^o V_1}{RV_2}\left(\frac{1}{T_m} - \frac{1}{T_m^o}\right) + \frac{\ln\phi_2}{m_2} + \left(\frac{1}{m_2} - \frac{1}{m_1}\right)\phi_1\right] = \phi_1^2\chi_{12} \quad (6)$$

If χ_{12} is assumed to be independent of the blend composition and the melting temperature depression is assumed to be independent of the morphological effects, a plot of the LHS of Eq. (6) against ϕ_1^2 yields a straight line, and χ_{12} is calculable from the slope. Fig. 7 was obtained using the appropriate numerical values for the various parameters for the PLLA–EVA85 blend: (T_m^o = 436 K, V_1 = 72.24 $cm^3\,mol^{-1}$, V_2 = 59.5 $cm^3\,mol^{-1}$, $m_1 = 8357$, $m_2 = 582$, $\rho_1 = 1.07\ g\,cm^{-3}$ $\rho_2 = 1.21\ g\,cm^{-3}$ and $\Delta H^o = 1600\ cal\,mol^{-1}$ [24], [25]). The interaction parameter between PLLA and EVA85 was thus founded to be -0.043, indicating the PLLA–EVA85 blend formed a thermodynamically stable homogeneous solution in the melt state.

The enthalpy of fusion of PLLA in the PLLA–EVA85 blend in Fig. 8 was obtained by DSC while the blend was scanned the second time. The enthalpy of fusion of PLLA crystallites in the blend was seen to decrease with an increase in the EVA85 content. Fig. 9 depicts the heat of fusion as a function of the blend composition obtained during the measurement of the equilibrium melting temperature. Contrary to the results in Fig. 8 the heat of fusion did not change much, as the EVA85 content and crystallization temperature were varied. Thus, the decrease in the crystallinity (Fig. 4) and the heat of fusion (Fig. 8) of PLLA crystallites with an increase in the EVA85 content could be due to the crystallization rate of PLLA being very slow and the crystallization being incomplete during the nonisothermal crystallization process in DSC. In fact, the enthalpy of fusion of the blend in the nonisothermal crystallization process was nearly constant and independent of the blend composition for the miscible blends of PHB–PEO [24], PHB–EVA85 [26] and PHB–poly(lactic acid-*co*-ethylene glycol-*co*-adipate) [27], where the crystallization of PHB was reasonably fast.

The radius of PLLA spherulites of the PLLA–EVA70 blend is plotted against the crystallization time in Fig. 10, for a blend crystallized at 105°C. Straight lines were obtained for all the blend compositions and the slopes were almost identical irrespective of the EVA70 content in the blend. Meanwhile, for the PLLA–EVA85 blend the slope decreased with an increase in the EVA85 content, as shown in Fig. 11. In Fig. 12 the spherulitic growth rates between 90°C and 125°C are shown for different blend compositions. The growth rate of the spherulite was decreased as the EVA85 content in the blend was increased, and the growth rate of PLLA spherulite was the highest at 105°C, regardless of the blend composition.

It is always necessary to investigate the presence of microheterogeneity even though the blend shows a single T_g and the melting temperature depression. The existence of microheterogeneity can be examined by the plot of log G' versus logG'' [28,29]. If such plot is dependent upon the temperature or shows inflection points, the blend contains microheterogeneity. Fig. 13 is the plot of logG' versus logG'' of the PLLA–EVA85 blend (50/50). A temperature-independent straight line was obtained between 150°C and 170°C, which undoubtedly means the PLLA–EVA85 (50/50) blend is miscible without any microscopic inhomogeneity.

PHB was also reported to show similar miscibility behavior toward EVA. PHB was immiscible with EVA70, while it was miscible with EVA85 [26]. In general, the window of the solubility parameter for the miscible polymer pairs is rather narrow. However, PVAc formed miscible or

Table 2
Tensile properties of the PLLA–EVA85 blends

Sample	Stress at break (kg mm^{-2})	Tensile modulus (kg mm^{-2})	Strain at break (%)
PLLA100	5.7	219	4.5
PLLA90	4.6	184	4.7
PLLA70	3.3	134	6.9
PLLA50	1.7	130	10.2
PLLA30	1.7	131	9.0
PLLA10	1.4	64	208.9
EVA85	1.4	62	244.9

compatible polymer blends with many different polymers of varying solubility parameter, including PLLA, PHB [32], poly(methyl methacrylate) [33], poly(ethyl acrylate) [34] and poly(butyl acrylate) [34]. The fact that EVA85 is miscible with both PHB and PLLA, whose hydrophilicities are widely different, may result from the high vinyl acetate content in EVA85.

Table 2 shows the breaking strength, modulus, and strain-at-break of the PLLA–EVA85 blend. The properties of PLLA alone were similar to those reported by Tsuji et al. [30] and Hiljanen-Vainio et al. [31]. As the EVA85 content was increased, breaking strength and modulus began to decrease sharply, which was followed by a rather slower decrease. On the other hand, strain-at-break was gradually increased up to 70 wt% of EVA85 and then suddenly increased at 90 wt% of EVA85.

Acknowledgements

This work was supported by the Korea Science and Engineering Foundation (94-0900-07-01-3).

References

[1] Zhang X, Goosen M, Wyss UP, Pichora D. J Macromol Sci, Rev Macromol Chem Phys 1993;C33 (1):81.
[2] Penning JP, Dijkstra H, Pennings AJ. Polymer 1993;34 (5):942.
[3] Vainionpaa S, Rokkanen P, Tormala P. Prog Polym Sci 1989;14:679.
[4] Heller J. Biomaterials 1980;1:51.
[5] Jakanicz TM, Nash HA, Wise DL, Gregory JB. Contraception 1973;8:227.
[6] Vert M, Christel P, Chabot F, Leyray J. In: Hastings GW, Ducheyne P. Macromolecular biomaterials. Boca Raton, FL: CRC Press, 1984:120–142.
[7] Miller RA, Brady JM, Cutright DE. J Biomed Mater Res 1977;11:711.
[8] Vert M, Chabot F, Leyray J, Christel P. Makromol Chem Suppl 1981;5:30.
[9] Chu CC. J Appl Polym Sci 1981;26:1727.
[10] Leenslag JW, Pennings AJ, Bos RM, Rozema FR, Boering G. Biomaterials 1987;8:311.
[11] Fukuzaki H, Yoshida M, Asano M, Kumakura M. Eur Polym J 1989;25 (10):1019.
[12] Reeve MS, McCarthy SP, Gross RA. Macromolecules 1993;26:888.
[13] Stevels WM, Bemard A, Van De Witte P, Dijkstra PJ, Feijen J. J Appl Polym Sci 1996;62:1295.
[14] Koyama N, Doi Y. Macromolecules 1996;29:5843.
[15] Nakayama A, Kawasaki N, Arvanitoyannis I, Iyoda J, Yamamoto N. Polymer 1995;36:1295.
[16] Gajria AM, Davé V, Gross RA, McCarthy SP. Polymer 1996;37:437.
[17] Li SM, Rashkov I, Espartero JL, Manolova N, Vert M. Macromolecules 1996;29:57.
[18] Zhang L, Xiong C, Deng X. Polymer 1996;37:235.
[19] Nolle AW. J Polym Sci 1950;5:1.
[20] Fox TG. Bull Am Phys Soc 1956;1:123.
[21] Hoffman JD, Weeks JJ. J Res Natl Bur Std 1962;66:13.
[22] Flory PJ. Principles of polymer chemistry. Ithaca, NY: Cornell University Press, 1953.
[23] Nishi T, Wang TT. Macromolecules 1975;8:909.
[24] Avella M, Martuscelli E. Polymer 1988;29:1731.
[25] Barham PJ, Keller A, Otun EL, Holmes PA. J Mater Sci 1984;19:2781.
[26] Yoon JS, Oh SW, Kim MN. Polymer 1998;39:2474.
[27] Yoon JS, Chang MC, Kim MN, Kang EJ, Kim C, Chin IJ. J Polym Sci, Polym Phys 1996;34:2543.
[28] Han CD, Kim JK. Polymer 1993;34:2533.
[29] Chauang HK, Han CD. J Appl Polym Sci 1984;29:2205.
[30] Tsuji H, Ikada Y. Polymer 1995;36:2709.
[31] Hiljanen-Vainio M, Varpomaa P, Seppälä J, Törmälä P. Macromol Chem Phys 1996;197:1503.
[32] Greco P, Martuscelli E. Polymer 1989;30:1475.
[33] Song M, Long F. Eur Polym J 1991;27:983.
[34] Krause S. Polymer–polymer compatibility. In: Paul DR, Newman S, editors. Polymer blends. New York: Academic Press, 1978 (and references therein).